NEURORADIOLOGY

Iran J Radiol. 2016 January; 13(1): e22144. DOI: 10.5812/iranjradiol.22144

Published online 2016 January 7. **Research Article**

Stereoscopic Display of the Peripheral Nerves at the Elbow Region Based on MR Diffusion Tensor Imaging with Multiple Post-Processing Methods

Wen Quan Ding,[1] Jian Hui Gu,[2] Yong Yuan,[3] and Dong Sheng Jin[3,*]

[1]Department of Hand Surgery, Ningbo No.6 Hospital, Ningbo University, Ningbo, China
[2]Department of Hand Surgery, Hand Surgery Research Center, Affiliated Hospital of Nantong University, Nantong University, Nantong, China
[3]Department of Radiology, Jiangsu Province Official Hospital, Jiangsu Jiankang Vocational College, Nanjing, China

*Corresponding author: Dong Sheng Jin, Department of Radiology, Jiangsu Province Official Hospital, Jiangsu Jiankang Vocational College, Nanjing, China. Tel: +86-02583712838-3067, Fax: +86-02586631726, E-mail: jindongshengnj@163.com

Received: July 18, 2014; **Revised:** August 23, 2014; **Accepted:** August 30, 2014

Abstract

Background: Peripheral nerves at the elbow region are prone to entrapment neuropathies and injuries. To make accurate assessment, clinicians need stereoscopic display of the nerves to observe them at all angles.

Objectives: To obtain a stereoscopic display of the peripheral nerves at the elbow region based on magnetic resonance (MR) diffusion tensor imaging (DTI) data using three post-processing methods of volume rendering (VR), maximum intensity projection (MIP), and fiber tractography, and to evaluate the difference and correlation between them.

Subjects and Methods: Twenty-four elbows of 12 healthy young volunteers were assessed by 20 encoding diffusion direction MR DTI scans. Images belonging to a single direction (anterior-posterior direction, perpendicular to the nerve) were subjected to VR and MIP reconstruction. All raw DTI data were transferred to the Siemens MR workstation for fiber tractography post-processing. Imaging qualities of fiber tractography and VR/MIP were evaluated by two observers independently based on a custom evaluation scale.

Results: Stereoscopic displays of the nerves were obtained in all 24 elbows by VR, MIP, and fiber tractography post-processing methods. The VR/MIP post-processing methods were easier to perform compared to fiber tractography. There was no significant difference among the scores of fiber tracking and VR/MIP reconstruction for single direction. The imaging quality scores of fiber tractography and VR/MIP were significantly correlated based on intraclass correlation coefficient (ICC) analysis (ICC ranged 0.709 - 0.901), which suggested that the scores based on fiber tractography and VR/MIP for the same sample were consistent. Inter- and intraobserver agreements were good to excellent.

Conclusion: Stereoscopic displays of the peripheral nerves at the elbow region can be achieved by using VR, MIP, and fiber tracking post-processing methods based on raw DTI images. VR and MIP reconstruction could be used as preview tools before fiber tracking to determine whether the raw images are satisfactory.

Keywords: Diffusion Tensor Imaging; Peripheral Nerves; Magnetic Resonance Imaging

1. Background

Peripheral nerves, especially those at the elbow region, such as the median nerve and ulnar nerve, are prone to entrapment neuropathies and injuries, such as cubital tunnel syndrome (1, 2), pronator teres syndrome (3), and nerve laceration (4). The traditional method used for evaluating these diseases with respect to preoperative diagnosis and postoperative rehabilitation is electrophysiological nerve conduction and electromyography; however, accurate evaluations using these methods largely depend on the operator's experience, and false negative results are common (5). A magnetic resonance (MR) image can display the soft tissue, including nerves, in T1 or T2 images, and the most commonly used method of MR for the diagnosis of peripheral nerve entrapment is to measure the cross sectional area (CSA) and T2 signal intensity, which cannot distinguish axonal injury from demyelination (6). Moreover, the continuity and integrity of a nerve can hardly be detected based on two-dimensional (2D) images. Therefore, obtaining a three-dimensional (3D) display of a nerve that can be observed at any angle is essential for clinicians to make accurate assessments.

Currently, the methods and sequences of MR neurography are mostly represented through diffusion tensor imaging (DTI). DTI with fiber tracking was the first method used to obtain a 3D view of the nerve, which was originally applied to image the central nervous system. Fiber tracking relies on the diffusion of water molecules contained within nerve fibers. Diffusion is less restricted in the direction parallel to the nerve fiber than that perpendicular to the fiber (possibly due to the layers of myelin). Using special fiber-tracking software to reconstruct the DTI data, it is possible to visualize the complete neural structure. In June 2004, Skorpil et al. (7) demon-

strated that peripheral nerves (the sciatic nerve in three healthy volunteers) could be imaged in vivo by using DTI with fiber tracking. This technique has now become the most widely used method for evaluating the status of the median nerves in carpal tunnel syndrome (8), providing non-invasive imaging of peripheral nerve regeneration (9-11), and characterizing the structure of the brachial plexus (12).

However, studies reporting the use of DTI with fiber tracking post-processing at the elbow region are scarce. The following drawbacks of using DTI for the elbow region, especially for the ulnar nerve, have been discussed: (i) it is superficial; (ii) close to the bone surface; and (iii) shows large angulations in the course of the nerve (13). Besides, these limitations of DTI with respect to specific anatomical characteristics at the elbow region, the technique itself has many limitations. First, the quality of tractography depends on the parameters used in the acquisition step, such as the coils used, positioning of the patient, and other parameters including the b-value and the number of diffusion directions. Chhabra et al. (14) suggested using joint-specific coils at the joint region. When using this type of hard coil, the elbow must be placed in the center of the magnetic field. To obtain this position, the subject must raise one hand above his/her head while in prone or supine position, which can be very uncomfortable. This leads to an increase in motion artifacts that impairs the imaging results. A flex coil can be used to decrease this effect. Second, during the post-processing phase before fiber tracking, the operator must choose a series of regions of interest (ROI), which depends on the operator's anatomical knowledge. Therefore, the choice of ROI may be partially subjective.

In addition to the DTI fiber tracking technique, a novel post-processing method to reconstruct DTI data was developed by Skorpil et al. (15) in 2007. They used the maximum intensity projection (MIP) technique to reconstruct sciatic nerves based on DTI images in a single direction and in all directions. Furthermore, based on preliminary experiments performed at the wrist region, we found that images of a single direction could also be reconstructed by using volume rendering (VR) and MIP. These two post-processing methods (VR and MIP) may offer a more convenient procedure for DTI because they do not require prior choice of ROIs.

2. Objectives

We predicted that the peripheral nerve at the elbow region could be three-dimensionally displayed based on the MR DTI data with multiple post-processing techniques. We aimed to determine whether the VR or MIP reconstruction for single direction would be more convenient than fiber tracking post-processing while acquiring approximate qualities of nerve imaging, and the consistency of VR/MIP and fiber tracking post-processing for the same sample.

3. Subjects and Methods

3.1. Study Subjects

The study had prior approval by our institutional review board and ethics committee, and all subjects provided informed consent prior to the study. The study protocol conforms to the ethical guidelines of the 1975 Declaration of Helsinki. A total of 24 elbows of 12 healthy, young volunteers were studied (six men, six women; age range 22 - 32 years). Nerves at the elbow region were analyzed, including the median nerve, ulnar nerve, and radial nerve. The exclusion criteria included general contraindications for MR imaging (MRI), a prior history of trauma or surgery of the elbow, presence of rheumatoid arthritis, and presence of space-occupying lesions at the elbow.

3.2. MR Imaging Protocol

The MR images were acquired with a Siemens Magnetom Verio 3T MRI scanner (Siemens Healthcare; Erlangen, Germany) using a 4-channal flex coil (flex small 4; Siemens). The MRI system's maximum field gradient amplitude was 45 mT/m with a slew rate of 200 T m^{-1} s^{-1}.

During the scan session, the soft coil was placed around the elbow, and then a polymer brace was placed on the whole upper limb in order to restrain movement. The upper limb was moved away from the body. The subject's upper extremity with the coil was immobilized with cushions, sandbags, and bandages. The elbow was then positioned to the center of the magnet bore. For imaging of the elbow, the subject was placed in the scanner in supine position (head first).

DTI was performed using an echo planar inversion recovery (EPIR) sequence (TR = 15,300 ms; TE= 92 ms; TI = 200 ms; FA = 90°; ETL = 1; FOV = 250 × 250 mm; scan matrix =128 × 128; average = 2) with 38 transversal slices of 3.0-mm thickness with no gap between the slices. Diffusion weighting with a b value of 1200 s/mm^2 was applied in 20 encoding diffusion directions. In addition to the diffusion-weighted images, a single reference image without diffusion weighting (b = 0 s/mm^2) was acquired. For anatomical reference, a T1-weighted image (TR = 700 ms; TE = 11 ms; FA = 150°; ETL = 3; thickness = 3 mm; gap = 0 mm; FOV = 140 × 140 mm; scan matrix = 320 × 240; average = 1) was acquired. The scanning times for DTI and T1-weighted image were 11 min 29 s and 2 min 1 s, respectively, for a total scan time of approximately 15 min.

3.3. VR and MIP Post-Processing

The raw DTI images were transferred automatically to the Siemens MR workstation (Siemens Syngo 3D). Table 1 shows the gradient table of DTI gradient with 20 diffusion directions. The X-axis represents the anterior–posterior direction, the Y-axis represents the left-right di-

rection, and the Z-axis represents the superior–inferior direction. Based on the gradient table of the DTI scan, direction 1 with coordinates (1, 0, 0) represents the anterior–posterior direction. Therefore, according to Skorpil et al. (15), the most suitable choice for single direction VR post-processing is direction 1, which is perpendicular to the nerves. The original DTI images usually contained a series of T2-weighted images (b = 0 s/mm^2), which were generated as the first series in the result chart. The optimal choice (direction 1) was the second series generated in the result chart. During VR/MIP reconstruction of images of direction 1, any high-signal noises of the veins or skin present in the reconstructed stereoscopic view were cut off in order to make the nerves as conspicuous as possible. One of the authors (Y.Y) was responsible for this part of the work.

Table 1. Gradient Table of DTI with Twenty Diffusion Directions

Direction No.	X [a]	Y [b]	Z [c]
0	0.000000	0.000000	0.000000
1 [d]	1.000000	0.000000	0.000000
2	0.000000	1.000000	0.000000
3	-0.031984	0.799591	0.599693
4	0.856706	0.493831	-0.148949
5	0.834429	0.309159	0.456234
6	0.834429	-0.309159	0.456234
7	0.856706	-0.493831	-0.148949
8	0.822228	0.000000	-0.569158
9	0.550834	0.425872	-0.717784
10	0.468173	0.834308	0.281963
11	0.515933	0.808894	0.281963
12	0.391890	0.515855	0.761785
13	0.478151	0.000000	0.878278
14	0.391890	-0.515855	0.761785
15	0.515933	-0.808894	0.281963
16	0.468173	-0.834308	-0.291108
17	0.550834	-0.425872	-0.717784
18	0.111012	-0.264029	-0.958105
19	0.111012	0.264029	-0.958105
20	0.031984	0.799591	-0.599693

[a] X-axis represents the anterior-posterior direction.
[b] Y-axis represents the left-right direction.
[c] Z-axis represents the superior-inferior direction.
[d] Direction 1 with the coordinates (1, 0, 0) represents the anterior-posterior direction.

3.4. Fiber Tractography

The raw DTI images were transferred to the Siemens MR workstation (Siemens Syngo Neuro 3D). Fiber tractography was then performed using a multiple seed ROI technique, which employed fiber assignment by continuous tracking. Seed ROIs were drawn freehand at three anatomical locations (level to the supracondylar humerus, olecranon, and proximal radioulnar joint) on the raw DTI images and reference T1-weighted images. ROIs were confined precisely to the nerve border to avoid partial volume artefacts and to exclude any surrounding structure from the seed ROIs. In this study, the fractional anisotropy (FA) threshold value was 0.2 and the angulation tolerance was 30°. The software's option "step length" was set to 0.47 mm. Another author (D.-S.J) was responsible for this part of the work.

3.5. Imaging Quality Evaluation

In order to compare the imaging quality among VR/MIP and fiber tractography, we created a custom evaluation scale to assess each nerve in VR/MIP and fiber tractography images. As to the scale setting, we read the study of Zhao et al. (16) for reference. We set the scale based on whether the target nerve could be shown and the length of the nerve was complete as follows: score of 2, the target nerve (the median, radial, or ulnar nerve) at the elbow region was clearly shown and the entire length of the nerve was visible throughout the entire scanning section; score of 1, the target nerve at the elbow region was clearly shown, but its length was incomplete; score of 0, the target nerve was invisible. Two authors (W.-Q.D and J.-H.G) were responsible for independently evaluating the imaging qualities according to this scale. One author (W.-Q.D) evaluated the imaging qualities again 4 weeks later.

3.6. Statistical Analysis

The imaging quality scores were expressed as medians with ranges and mean with SD. For each nerve, scores of VR/MIP reconstruction of the single direction and fiber tracking were compared using Friedman test. Differences were considered significant when P values were less than 0.05. Intraclass correlation coefficient (ICC) analysis was used to compare the correlation of the imaging quality scores for each nerve among VR/MIP and fiber tractography. Inter- and intraobserver agreements for evaluation scores were calculated by using the kappa statistic. Kappa values of 0 - 0.20 were considered to indicate poor agreement; 0.21 - 0.40, fair agreement; 0.41 - 0.60, moderate agreement; 0.61 - 0.80, good agreement; and 0.81 - 1.00, excellent agreement. Statistical analysis was performed by one author (J.-H.G) using SPSS statistical software, ver. 21 (IBM Corp. Released 2012. IBM SPSS Statistics for Windows, Armonk, NY).

4. Results

All 24 elbows of the 12 young volunteers were tested, and stereoscopic displays of the nerves were obtained by using VR, MIP, and fiber tractography post-processing methods (Figure 1). For most elbows of volunteers, three main nerves could be seen clearly (Figure 1), whereas only one nerve could be detected in other individual cases (Figure 2). Owing to the relatively simple and direct operations enabled without requiring ROIs selection, the VR and MIP post-processing methods were easier to perform compared to fiber tractography. VR/MIP reconstructions for single direction images and fiber tracking evaluation scores for each target nerve are listed in Table 2, which did not differ significantly ($P > 0.05$). The imaging quality scores of fiber tractography and VR/MIP were significantly correlated based on intraclass correlation coefficient (ICC) analysis (ICC ranged 0.709 - 0.901), which suggested good consistency between the scores obtained based on the fiber tractography and VR/MIP for the same sample. The κ values of inter- and intraobserver agreements ranged 0.674 - 0.909, which showed good to excellent agreements.

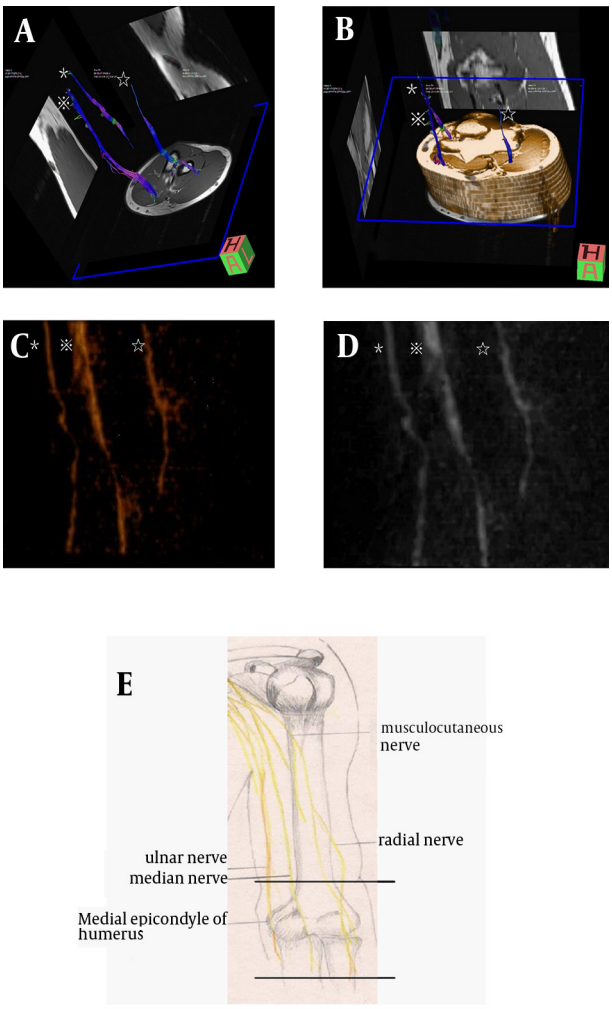

Figure 1. Fiber tractography and VR/MIP reconstruction of nerves from DT. The median nerve (※) radial nerve (☆), and ulnar nerve (＊) can be seen clearly. A, Fiber tractography. B, Fiber tractography of DTI with reference of T1-weighted images. C, VR reconstruction. D, MIP reconstruction. E, Reference picture of the three main nerves at the elbow region. The scanned section is located between the two parallel lines.

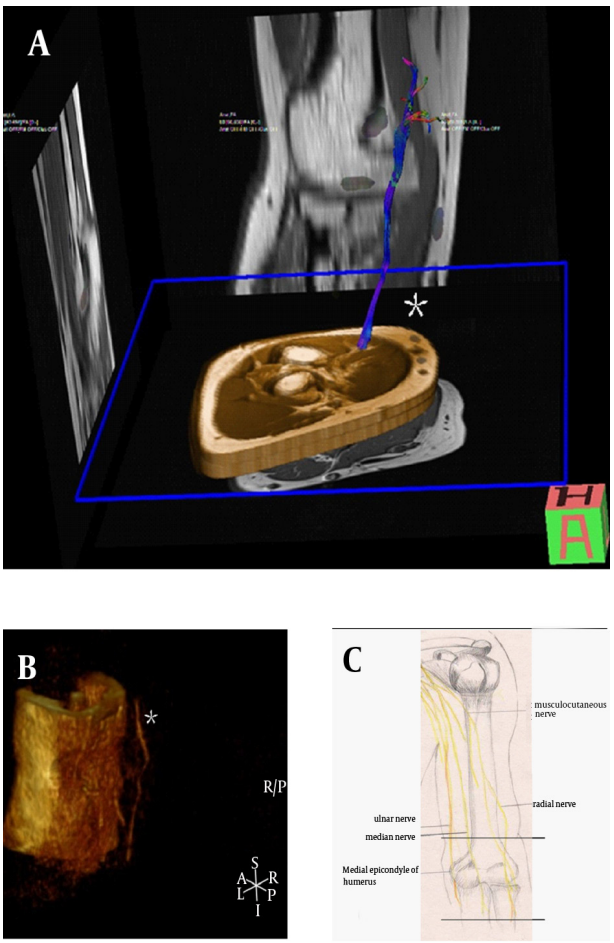

Figure 2. Fiber tractography and VR/MIP reconstruction of nerves from DTI. A, Fiber tractography. Only the ulnar nerve (＊) can be seen clearly, whereas the median nerve and radial nerve cannot be tracked. B, VR reconstruction (without noise removal). Only the ulnar nerve (＊) can be seen, which is located outside of the outline of the elbow. The median and radial nerve are covered by the outline of the elbow. C, Reference picture

Table 2. Evaluation Scores for Each Target Nerve Based on VR/MIP Reconstructions for Single Direction Images and Fiber Tracking [a]

Median Nerve	VR	MIP	FT	P Value [b]	ICC	κ1	κ2
Ob1							
Mean. (SD)	1.75 (0.532)	1.79 (0.509)	1.83 (0.482)			0.674	
Median. (range)	2 (0 - 2)	2 (0 - 2)	2 (0 - 2)	0.368	0.838		
Ob2							
Mean. (SD)	1.75 (0.532)	1.79 (0.509)	1.79 (0.509)				0.83
Median. (range)	2	2 (0 - 2)	2 (0 - 2)	0.779	0.79		
Ob2 Sec.							
Mean.(SD)	1.71 (0.550)	1.75 (0.532)	1.79 (0.509)				
Median.(range)	2 (0 - 2)	2 (0 - 2)	2 (0 - 2)	0.223	0.901		
Ulnar Nerve							
Ob1							
Mean. (SD)	1.38	1.42 (0.584)	1.46 (0.588)			0.711	
Median. (range)	1	1 (0 - 2)	1.50 (0 - 2)	0.368	0.877		
Ob2							
Mean. (SD)	1.54 (0.509)	1.54 (0.509)	1.46 (0.588)				0.733
Median. (range)	2 (1 - 2)	2 (1 - 2)	1.5 (0 - 2)	0.513	0.709		
Ob2 Sec							
Mean. (SD)	1.38 (0.576)	1.54 (0.509)	1.46 (0.588)				
Median. (range)	1 (0 - 2)	2 (1 - 2)	1.5 (0 - 2)	0.135	0.736		
Radial Nerve							
Ob1							
Mean. (SD)	1.04 (0.690)	1.04 (0.690)	0.92 (0.654)			0.909	
Median. (range)	1 (0 - 2)	1 (0 - 2)	1 (0 - 2)	0.105	0.88		
Ob2							
Mean. (SD)	1.04 (0.690)	1.17 (0.761)	0.96 (0.690)				0.845
Median. (range)	1 (0 - 2)	1 (0 - 2)	1 (0 - 2)	0.066	0.812		
Ob2 Sec							
Mean. (SD)	1.08 (0.717)	1.21 (0.721)	1.00 (0.722)				
Median. (range)	1 (0 - 2)	1 (0 - 2)	1 (0 - 2)	0.066	0.815		

[a] Abbreviations: FT, fiber tractography; ICC, intraclass correlation coefficient; κ1, interobserver κ value; κ2, intraobserver κ value; Ob1, observer 1; Ob2, observer 2; Ob2 Sec., observer 2 second time.
[b] P Values were calculated by Friedman test.

5. Discussion

In this study, we found that some images belong to a single direction (perpendicular to the nerve) after DTI scan could be used for VR or MIP reconstruction to display the peripheral nerves clearly. This method is similar to unidirectional diffusion-weighted MR neurography (DW-MRN) (16, 17). The difference of applied diffusion directions between DTI and DW-MRN scans is that DTI scan can select many non-parallel diffusion directions, and the data can be used for fiber tracking and measuring the FA, apparent diffusion coefficient (ADC) value, while DW-MRN can choose fewer number of diffusion directions, increase the excitation frequency so the scan time is shorter, and signal-to-noise ratio increased for better MIP or VR display. Studies of Zhao et al. (16) and Takahara et al. (17) indicated when they applied diffusion direction which is perpendicular to the nerve axons, the water molecular diffusion in the nerve was restricted, so the nerve tissue could all be imaged and showed high signal. We speculated that in DTI scan, the data collected from the perpendicular direction may play an important role in calculating FA value, which is the key parameter for fiber tracking. Thus, VR and MIP reconstruction of a single direction (anterior-posterior direction, perpendicular to the nerve) could predict the imaging quality of fiber tractography.

The results of this study raise an important and essential question: under the same experimental conditions, why do the results show variation among different healthy volunteers? For some elbows of volunteers, three main nerves could be seen clearly (Figure 1), whereas only one nerve could be detected in other cases (Figure 2). Besides the reasons of anatomical characteristics at the elbow region and the limitations of the technique, one possible explanation for this variation is that slight movement of the limb is the key factor affecting imaging quality. In the image shown in Figure 2, only the ulnar nerve is visible from VR reconstruction. The ulnar nerve is located outside of the outline of the elbow. The median nerve and radial nerve are covered by the outline of the elbow, which suggests that the signal values of the nerve fibers were calculated incorrectly, thereby affecting fiber tracking.

VR and MIP post-processing are more convenient to obtain compared to fiber tracking. The selection of ROIs is not required, which prevents subjective factors from influencing the results. The ICC analysis result suggested that scores based on fiber tractography and VR/MIP for the same samples were highly consistent. Therefore, VR and MIP reconstruction can be used as a simple preview tool before performing complicated fiber tracking. During the DTI scanning process using Siemens Magenetom Verio 3T MRI scanner, the DTI original images are generated in the order of the gradient table (Table 1) from direction 1 to direction 20, and from average 1 to average 2. The images belonging to direction 1 of average 1 will be generated within the first few seconds, and then VR and MIP post-processing can be immediately performed to observe whether or not the nerve is displayed. If the nerves display, then, a scan with more directions and more averages should be continued for fiber tracking. If the nerves do not display, the scan should be terminated, and more measures for restricting movement of the elbow should be adopted. Using this method could help save a lot of time to the benefit of both the clinician and the patient.

Some potential applications of VR and MIP reconstruction include evaluation of the continuity and integrity of the nerve as well as detection of abnormal morphology, whereas the application of fiber tracking is specific to assessing the status of axons. According to Sunderland's nerve injury classification (18), grade I, grade II, and some grade III injuries (axons or endoneurial tube disruptions) do not require surgical exploration, whereas grade IV-VI injuries (perineurium or epineurium damages, defects, or mixed injuries) do require surgical exploration as soon as possible. Therefore, VR and MIP reconstruction might be able to show more details of damaged nerves, which unlike fiber tracking, do not only focus on the axons. Background tissue also can be reconstructed as reference landmark to show the damage site of nerve more clearly.

Cubital tunnel syndrome is the second-most common nerve compression syndrome after carpal tunnel syndrome. Injury of the ulnar nerve at the elbow region is also common, because it is superficial and close to the bone surface. Stereoscopic display of the nerves at the elbow region can help the clinician understand the morphology of the target nerve. For example, in nerve entrapment patients, nerves can be detected as the features of increasing CSA and flatten ratio (FR), which can be observed more easily in stereoscopic displays compared with conventional 2D images. By using these methods with the addition of FA and ADC value measurements, DTI appears to be a promising tool for future evaluations of the severity and rehabilitation of ulnar neuropathy.

This study has considerable limitations that are worth noting. First, due to the limited choice of equipment and coil, the parameters and coil of the DTI scan at the elbow region did not reach adequate optimization. Second, the measures adopted for restricting slight movement of the limb were not highly efficient.

Stereoscopic displays of the peripheral nerve at the elbow region were achieved by using VR, MIP, and fiber tracking post-processing methods based on raw DTI images. The scores based on VR/MIP and fiber tracking post-processing had good consistency for the same samples indicating that VR and MIP reconstruction for single direction could be used as preview tools before fiber tracking to determine whether the raw images are satisfactory.

Acknowledgements

We thank Dr. Wang Xin (Department of Hand Surgery, Ningbo No.6 Hospital) for communicating with the grants supporter.

Authors' Contributions

Wen Quan Ding carried out the design of the study and was responsible for evaluating fiber tractography qualities. Jian Hui Gu was responsible for evaluating VR/MIP qualities and statistical analysis. Dong sheng Jin and Yong Yuan were responsible for DTI scan and post-processing.

Funding/Support

Special project for major diseases' prevention and treatment, national health and family planning commission of the people's republic of China

References

1. Soltani AM, Best MJ, Francis CS, Allan BJ, Panthaki ZJ. Trends in the surgical treatment of cubital tunnel syndrome: an analysis of the national survey of ambulatory surgery database. *J Hand Surg Am.* 2013;**38**(8):1551–6.
2. Kroonen LT. Cubital tunnel syndrome. *Orthop Clin North Am.* 2012;**43**(4):475–86.
3. Zancolli ER, Zancolli P, Perrotto CJ. New mini-invasive decompression for pronator teres syndrome. *J Hand Surg Am.* 2012;**37**(8):1706–10.
4. Pfaeffle HJ, Waitayawinyu T, Trumble TE. Ulnar nerve laceration and repair. *Hand Clin.* 2007;**23**(3):291–9.
5. Yoon JS, Walker FO, Cartwright MS. Ulnar neuropathy with normal electrodiagnosis and abnormal nerve ultrasound. *Arch Phys Med Rehabil.* 2010;**91**(2):318–20.
6. Kang S, Kim SH, Yang SN, Kim SJ, Yoon JS. Factors affecting ultraso-

nographic findings of the ulnar nerve in ulnar neuropathy at the elbow. *J Neur Sci.* 2013;**333**:e450.
7. Skorpil M, Karlsson M, Nordell A. Peripheral nerve diffusion tensor imaging. *Magn Reson Imaging.* 2004;**22**(5):743–5.
8. Hiltunen J, Kirveskari E, Numminen J, Lindfors N, Goransson H, Hari R. Pre- and post-operative diffusion tensor imaging of the median nerve in carpal tunnel syndrome. *Eur Radiol.* 2012;**22**(6):1310–9.
9. Li X, Chen J, Hong G, Sun C, Wu X, Peng MJ, et al. In vivo DTI longitudinal measurements of acute sciatic nerve traction injury and the association with pathological and functional changes. *Eur J Radiol.* 2013;**82**(11):e707–14.
10. Takagi T, Nakamura M, Yamada M, Hikishima K, Momoshima S, Fujiyoshi K, et al. Visualization of peripheral nerve degeneration and regeneration: monitoring with diffusion tensor tractography. *Neuroimage.* 2009;**44**(3):884–92.
11. Lehmann HC, Zhang J, Mori S, Sheikh KA. Diffusion tensor imaging to assess axonal regeneration in peripheral nerves. *Exp Neurol.* 2010;**223**(1):238–44.
12. Mallouhi A, Marik W, Prayer D, Kainberger F, Bodner G, Kasprian G. 3T MR tomography of the brachial plexus: structural and microstructural evaluation. *Eur J Radiol.* 2012;**81**(9):2231–45.
13. Ohana M, Moser T, Meyer N, Zorn PE, Liverneaux P, Dietemann JL. 3T tractography of the median nerve: optimisation of acquisition parameters and normative diffusion values. *Diagn Interv Imaging.* 2012;**93**(10):775–84.
14. Chhabra A, Flammang A, Padua AJ, Carrino JA, Andreisek G. Magnetic resonance neurography: technical considerations. *Neuroimaging Clin N Am.* 2014;**24**(1):67–78.
15. Skorpil M, Engstrom M, Nordell A. Diffusion-direction-dependent imaging: a novel MRI approach for peripheral nerve imaging. *Magn Reson Imaging.* 2007;**25**(3):406–11.
16. Zhao L, Wang G, Yang L, Wu L, Lin X, Chhabra A. Diffusion-weighted MR neurography of extremity nerves with unidirectional motion-probing gradients at 3 T: feasibility study. *AJR Am J Roentgenol.* 2013;**200**(5):1106–14.
17. Takahara T, Hendrikse J, Kwee TC, Yamashita T, Van Cauteren M, Polders D, et al. Diffusion-weighted MR neurography of the sacral plexus with unidirectional motion probing gradients. *Eur Radiol.* 2010;**20**(5):1221–6.
18. Sunderland S. A classification of peripheral nerve injuries producing loss of function. *Brain.* 1951;**74**(4):491–516.